

DIFFRACTION OF ELECTROMAGNETIC WAVES BY
IMPEDANCE SLITS AND STRIPS

A THESIS SUBMITTED TO
THE GRADUATE SCHOOL OF NATURAL AND APPLIED SCIENCES
OF
ÇANKAYA UNIVERSITY

BY

GALİP ÇAĞLAR COŞKUN

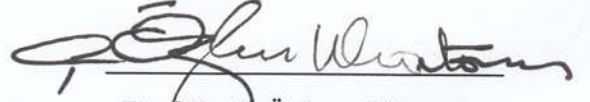
IN PARTIAL FULFILLMENT OF THE REQUIREMENTS
FOR
THE DEGREE OF MASTER OF SCIENCE
IN
ELECTRONIC & COMMUNICATION ENGINEERING

JUNE 2008

Title of the Thesis : **Diffraction of Electromagnetic Waves by Impedance Slits and Strips**

Submitted by **Galip Çağlar Coşkun**

Approval of the Graduate School of Natural and Applied Sciences, Çankaya University



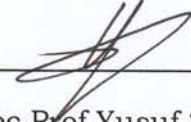
Prof. Dr. C. Özhan Uluatam
Acting Director

I certify that this thesis satisfies all the requirements as a thesis for the degree of Master of Science



Prof. Dr. Yahya Kemal Baykal
Head of Department

This is to certify that we have read this thesis and that in our opinion it is fully adequate, in scope and quality, as a thesis for the degree of Master of Science

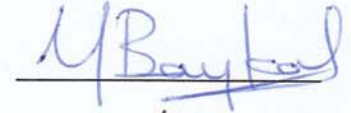


Assoc. Prof. Yusuf Ziya Umul
Supervisor

Examination Date : 11. 06. 2008

Examining Committee Members :


Prof. Dr. Yahya Kemal Baykal (Çankaya Univ.)



Assoc. Prof. Yusuf Ziya Umul (Çankaya Univ.)



Asst. Prof. Dr. Aysel Şafak (Başkent Univ.)



STATEMENT OF NON-PLAGIARISM

I hereby declare that all information in this document has been obtained and presented in accordance with academic rules and ethical conduct. I also declare that, as required by these rules and conduct, I have fully cited and referenced all material and results that are not original to this work.

Name, Last Name : Galip Çağlar Coşkun

Signature : 

Date : 11 . 06 . 2008

ABSTRACT

DIFFRACTION OF ELECTROMAGNETIC WAVES BY IMPEDANCE STRIPS AND SLITS

Coşkun, Galip Çağlar

M.S.c., Department of Electronic & Communication Engineering

Supervisor : Assoc.Prof.Dr.Yusuf Ziya Umul

June 2008, 51 pages

In this thesis, diffraction process of electromagnetic waves by strips and slits will be examined by using the methods of the physical optics (PO) and modified theory of physical optics (MTPO) that have impedance boundary conditions on them. The integral will be evaluated by using the methods of stationary phase and edge point. The obtained solutions will be compared plotted numerically by using MATLAB.

Keywords : Electromagnetic diffraction, physical optics, modified theory of physical optics

ÖZ

EMPEDANS ŞERİTLERİ VE YARIKLARINDAN ELEKTROMANYETİK DALGALARIN KIRINIMI

Coşkun, Galip Çağlar

Yükseklisans, Elektronik ve Haberleşme Mühendisliği Anabilim Dalı

Tez Yöneticisi : Doç.Dr.Yusuf Ziya Umul

Haziran 2008, 51 sayfa

Bu tezde, fiziksel optik (PO) ve fiziksel optiğin değiştirilmiş teorisi (MTPO) metotları kullanılarak elektromanyetik dalgaların şeritler ve yarıklardan kırınımı, empedans sınır koşullarında incelenecektir. İntegraller stasyonel faz ve köşe nokta metotları kullanılarak hesaplanacaktır. Elde edilen sonuçlar MATLAB programıyla sayısal olarak karşılaştırılarak çizilecektir.

Anahtar Kelimeler : Elektromanyetik kırınım, fiziksel optik, fiziksel optiğin değiştirilmiş teorisi

ACKNOWLEDGMENTS

This thesis is dedicated to my family... To my mother, for bringing me up with all the best features I have; my father, for being my greatest support in every field of life; my sister, for being my inspiration and bringing joy to my life.

I would like to thank my advisor Assoc.Prof.Dr.Yusuf Ziya Umul for all his help and guidance in my studies for these two years. His positive attitude and encouragement played a very major role in my achievements and in the completion of this graduate study.

TABLE OF CONTENTS

| | |
|--|------|
| STATEMENT OF NON PLAGIARISM..... | iii |
| ABSTRACT..... | iv |
| ÖZ..... | v |
| ACKNOWLEDGMENTS..... | vi |
| TABLE OF CONTENTS | vii |
| LIST OF FIGURES..... | viii |
| CHAPTERS: | |
| 1. INTRODUCTION | 1 |
| 1.1 Geometrical Theory of Diffraction (GTD)..... | 2 |
| 1.2 Physical Optics | 4 |
| 1.3 Objectives of the Study..... | 7 |
| 2. SCATTERING FROM A PEC PARALLEL PLATE | 8 |
| 2.1 Scattering Geometry..... | 8 |

| | |
|---|----|
| 2.2 PO Solution of the Problem..... | 9 |
| 3. SCATTERING FROM IMPEDANCE SLIT..... | 20 |
| 3.1 Scattering Mechanisms | 20 |
| 3.2 PO Solution of the Problem..... | 21 |
| 4. NUMERICAL RESULTS | 28 |
| 5. CONCLUSIONS..... | 34 |
| REFERENCES | R1 |
| APPENDICESY: | |
| A. MATLAB Programme for Geometry in Chapter 2 | A1 |
| B. MATLAB Programme for Geometry in Chapter 3 | B1 |

LIST OF FIGURES

| | |
|---|----|
| Figure 1.1 Categories within Computational Electromagnetics..... | 5 |
| Figure 2.1 Plane Wave in a Parallel-Plate Guide..... | 8 |
| Figure 2.2 Aperture Geometry..... | 15 |
| Figure 3.1 Geometry of Second Problem..... | 20 |
| Figure 3.2 Geometry of the Impedance Slit..... | 24 |
| Figure 4.1 Scattered field for geometry of Fig. 2.1..... | 28 |
| Figure 4.2 The effect of impedance half planes to the radiating fields for the geometry of Fig. 3.1..... | 29 |
| Figure 4.3 Radiated field for geometry of Fig. 3.1..... | 31 |
| Figure 4.4 Radiated field for geometry of Fig. 3.1..... | 33 |

CHAPTER 1

INTRODUCTION

In accordance with Maxwell's equations and the corresponding boundary conditions, when electromagnetic field illuminates a perfectly conducting body, electric and magnetic currents are induced on the body. As new sources and generate an electromagnetic field of their own, the currents induced on the surface act. This field is the scattered field and is radiated in space as a function of the shape of the object, frequency and polarization of the incoming wave.

In this thesis, the main idea is focused on diffraction process of electromagnetic waves by strips and slits. Various calculation techniques are available for high-frequency scattering problems. A brief review of widely used high frequency techniques and their calculation procedures in general will be given in this introductory chapter.

The total electromagnetic field originated by a source may be expressed as the superposition of the reflected field, diffracted field and incident field in the high frequency regime. Incident and reflected fields may be calculated through geometrical optics (GO), which is the high frequency limit of zero wavelength and in which the scattering phenomenon is treated by classical ray tracing of incident, reflected and transmitted rays.

Young conceived the phenomenon of diffraction who described the source of this field as an interaction between all incremental elements of the edge. It is advocated by Young that interaction of different edge elements

with each other and with the GO field produces the observed interference pattern for the total field. To date, many high-frequency edge diffraction techniques have been developed to calculate the diffracted fields. Keller's Geometrical Theory of Diffraction (GTD) and Utimtsev's Physical Theory of Diffraction (PTD) are the most well known edge-diffraction techniques. Versions of Keller's GTD improved Uniform Theory of Diffraction (UTD) of The Ohio State University and Uniform Asymptotic Theory (UAT) of University of Illinois. Detailed information on these techniques can be found in [1] and [2].

1.1. Geometrical Theory of Diffraction (GTD)

A class of diffracted rays are introduced systematically depending on the concepts of GO in GTD. These diffracted rays exist in addition to the usual incident, reflected and transmitted rays of GO. On account of stationary points on the edge and superposing the contributions of all stationary points, GTD is based on determining the fields. Fields originating from points other than stationary points are assumed to be cancelling each other. The field originating from a stationary point is simply the product of four factors:

- (1) The value of the incident field at the scattering center,
- (2) The diffraction coefficient,
- (3) The divergence factor,
- (4) The phase factor.

The overall field at the observation point is found by adding to diffracted field the Geometrical Optics (GO) field or Physical Optics (PO) field according to whether GTD or PTD is being employed.

GTD fails within the transition regions adjacent to the shadow boundaries, since it is purely an optical theory. This failure of GTD can be overcome through the use of uniform ray techniques based on UTD and UAT. The GTD, UTD, and UAT all generally fail in ray caustic regions. The situations can be listed as follows (when these techniques are not applicable):

(1) If an infinite number of rays pass through the observation point, the total field cannot be obtained numerically. In such a case, the observation point is said to be a caustic. In this case total field obtained by using ray-optical techniques diverges.

(2) When the observation point is located at a point near a caustic, phase variation is so slow that destructive interference, which is the initial assumption for non-stationary points, is not realized sufficiently. In this case ray-optical techniques can be applied but they produce inaccurate results.

(3) If no stationary points exist, the observation point is outside the Keller cone and no rays pass through the observation point. Keller cone is the cone with the tip at the edge point, sides making the same angle with the edge tangent as the one that the incident ray makes with the edge tangent, but in the opposite direction. This case might occur when there are corners in the edge curve. Diffraction from corners can be calculated using corner diffraction coefficients formulated for GTD [1]. Corner diffraction coefficients are based on heuristic modifications of the wedge or half-plane solutions. An empirical corner diffraction coefficient for PTD is reported by Hansen [3].

Other than the problematic cases listed above, there may still be another problem even if isolated stationary points can be identified. The ray-optical techniques cannot be applied if the amplitude of the incident field changes rapidly along the edge.

Using the method of Equivalent Edge Currents (EEC) for edge-scattered fields and PO method for surface-scattered fields are the solution to these discrepancies. PTD is based in this approach. Being a correcting extension to GO, PTD is a correcting contribution to PO, just like GTD. PTD corrects the inaccurate diffraction coefficient obtained from the PO surface integration for edged bodies. PO overcomes the catastrophe of the infinities of GO by approximating the induced surface currents and integrating them to obtain the scattered field. Due to the fact that the induced fields remain finite, the scattered fields are finite as well. The scattering structure is first described in terms of the coordinates of a large number of points on the surface to calculate the PO-scattered field.

1.2. Physical Optics (PO)

The method of moments (MoM) and finite difference time-domain (FD-TD) are two numerical methods in computational electromagnetics (CEM) in antenna analysis and design. Whereas the potential of the latter in antenna work has only begun to be realized more recently, use of the former has been well established for several decades.

CEM is broadly defined as the discipline that intrinsically and routinely involves the use of a digital computer to obtain numerical results for electromagnetic problems. It is a third tool available to electromagnetics engineers, the other two being mathematical analysis, and experimental observation. It is not uncommon to verify analysis results and CEM results with experimental results, and also not is it uncommon to employ analysis and/or CEM to understand experimental results.

There are various ways to classify the assortment of techniques in CEM. Here, we choose to divide CEM into two major categories: numerical methods and high-frequency or asymptotic methods as shown in Fig. 1.1.

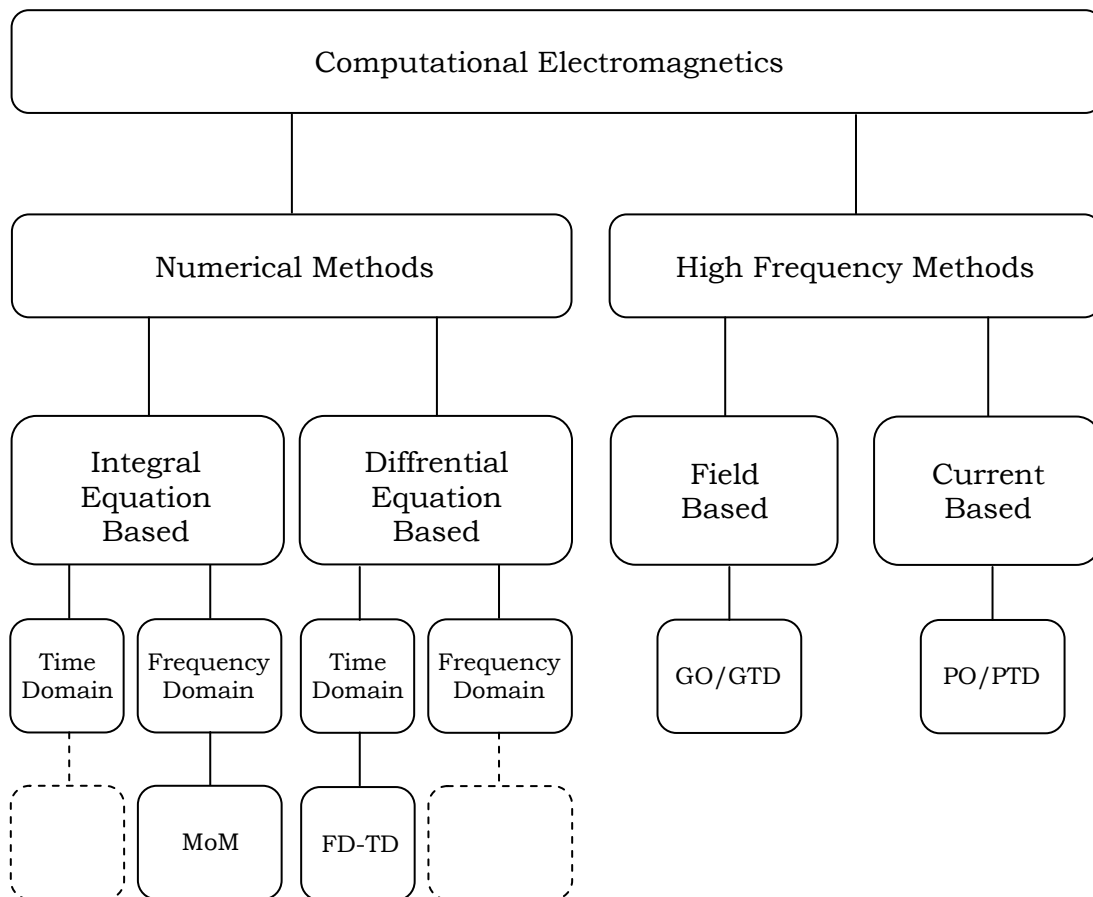


Figure 1.1. Categories within computational electromagnetics.

Current-based methods are physical optics and its extension to include diffraction. A physical optics current, in many conditions, is insufficient to produce accurate fields from a radiating object and it is essential to include another current called the non-uniform current. If a field based or a current based method is to be used on the specific application, the non-uniform current, when added to the physical optics current, permits an accurate representation of the fields to be obtained. If a field based or a current-based method is to be used relies on the specific application [4].

The edge diffracted fields from a PEC half plane is evaluated for Modified theory of physical optics (MTPO). The MTPO was developed by Umul which is able to obtain a surface current, will give the scattered

waves, but there occurs a problem when a second face, having the same or different boundary conditions, is taken into account as in wedge type problems. New surface currents are evaluated by considering the exact solution of the PEC wedge problem for taking into account the interaction of the surfaces [5].

The physical theory of diffraction (PTD) which is based on defining a non-uniform current component, which gives the high frequency asymptotic solution of diffraction problems, when added to the well known PO current, was developed by Ufimtsev in 1950's [6]. Ufimtsev suggested that the non-uniform field component is the result of the fringe currents, which flow on the discontinuity of the scatterer [7]. PTD is not described in detail expression which is given by Ufimtsev for these current components, depends on the evaluation of the fringe current or edge wave. Some of the weak points of PTD are studied in [8],[9]. In order to expand the method as incremental length diffraction coefficients (ILDC) of Mitzner and Michaeli's equivalent edge currents, other variations of PTD were improved. Ando introduced modified edge representation line integrals, executed an interesting approach to PTD.

As we see the differences between the methods of PTD and MTPO, MTPO considers a complementary aperture surface as an addition to the surface of the scatterer. This action provides to evaluate the total scattered fields. In other way PTD takes into account only the fringe current, which flows on the edge of the scatterer and uses it to correct the PO current which exists on the surface of the scatterer. PTD also needs the exact solution of the canonical diffraction problems in order to evaluate the fringe currents whereas MTPO uses its axioms in order to define pseudo-surface currents. It is shown in [10] that the diffraction coefficients of the geometrical theory of diffraction (GTD), can be obtained asymptotically from the MTPO integrals which is a high frequency asymptotic method by using this approach.

1.3. Objectives of the Study

In this thesis, diffraction process of electromagnetic waves by strips and slits will be examined by using the methods of the physical optics (PO) and modified theory of physical optics (MTPO) that have impedance boundary conditions on them. The integral will be evaluated by using the methods of stationary phase and edge point. The obtained solutions will be compared plotted numerically by using MATLAB. These concepts are presented in more detail in Chapter 2 and in Chapter 3.

CHAPTER 2

SCATTERING FROM A PEC PARALLEL PLATE

2.1. Scattering Geometry

Plane wave in a parallel-plate guide configuration is depicted in Fig. 2.1. Plane wave is guided in the y direction, but does so by means of a progression of zig-zag reflections at the upper and lower plates.

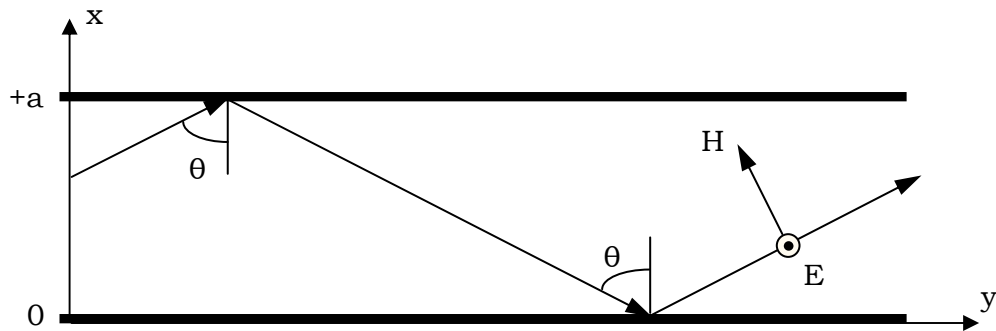


Figure 2.1. Plane wave in a parallel-plate guide.

The transverse electric (TE) mode is identified when \vec{E} is perpendicular to the plane of incidence; this positions \vec{E} parallel to the transverse plane of the waveguide [11].

Note, for example, that with \vec{E} in the z direction, \vec{H} will have x and y components.

$$\begin{aligned} E_x &= 0 & H_x &\neq 0 \\ E_y &= 0 & H_y &\neq 0 \\ E_z &\neq 0 & H_z &= 0 \end{aligned} \quad (2.1)$$

Parallel plates are illuminated by a plane wave. Assuming $e^{j\omega t}$ time dependence and suppressing it.

2.2. PO Solution of the Problem

The electric and magnetic field components of the plane wave are given by

$$\vec{E}_i = \vec{e}_z E_i \sin \frac{\pi}{a} x e^{-jk y} \quad (2.2)$$

where k is wave number which can be expressed as $k = \frac{\omega \mu}{Z_0}$ and

$$\vec{H}_i = -\frac{1}{j\omega\mu_0} \nabla \times \vec{E}_i \quad (2.3)$$

where ω is period and μ_0 is permeability of the material. $\nabla \times \vec{E}_i$ is the rotational operation on incident electrical field. Incident magnetic field can be calculated as

$$\vec{H}_i = -\frac{1}{j\omega\mu_0} \begin{vmatrix} \vec{e}_x & \vec{e}_y & \vec{e}_z \\ \frac{\partial}{\partial x} & \frac{\partial}{\partial y} & \frac{\partial}{\partial z} \\ 0 & 0 & E_{i_z} \end{vmatrix} \quad (2.4)$$

by taking the rotational operation in Eq.(2.3)

$$\vec{H}_i = -\frac{1}{j\omega\mu_0} \left(\vec{e}_x \frac{\partial E_{i_z}}{\partial y} - \vec{e}_y \frac{\partial E_{i_z}}{\partial x} \right) \quad (2.5)$$

Derivatives of incident electrical field are calculated and inserted into Eq.(2.5) as

$$\vec{H}_i = -\frac{1}{j\omega\mu_0} \left[\vec{e}_x (-jkE_i \sin \frac{\pi}{a} x e^{-jky}) + \vec{e}_y (-\frac{\pi}{a} E_i \cos \frac{\pi}{a} x e^{-jky}) \right] \quad (2.6)$$

and can be simplified as

$$\vec{H}_i = \vec{e}_x \frac{kE_i}{\omega\mu_0} \sin \frac{\pi}{a} x e^{-jky} + \vec{e}_y \frac{\pi E_i}{j\omega\mu_0 a} \cos \frac{\pi}{a} x e^{-jky}. \quad (2.7)$$

Equation (2.7) can be rearrange by $1/Z_0 = k/\omega\mu_0$, can given as

$$\vec{H}_i = \vec{e}_x \frac{E_i}{Z_0} \sin \frac{\pi}{a} x e^{-jky} + \vec{e}_y \frac{\pi E_i}{jkZ_0 a} \cos \frac{\pi}{a} x e^{-jky} \quad (2.8)$$

by using the formula of wave number k. Total scattered field at the aperture of the parallel plate can be calculated by using the PO method. The current induced by the incident magnetic field is considered. This surface current flows only on the illuminated surfaces of parallel plates. The field at the aperture region can also be obtained by integrating this current.

The electrical field at the aperture can be introduced as

$$\vec{E}_a = \vec{E}_i \Big|_{y'=0} \quad (2.9)$$

and can be calculated as

$$\vec{E}_a = \vec{e}_z E_i \sin \frac{\pi}{a} x' \quad (2.10)$$

using Eqs.(2.2) and (2.9), and the magnetic field at the aperture can be written as

$$\vec{H}_a = \vec{H}_t|_{y'=0} \quad (2.11)$$

and can be calculated as

$$\vec{H}_a = \vec{e}_x \frac{E_i}{Z_0} \sin \frac{\pi}{a} x' + \vec{e}_y \frac{\pi E_i}{jkZ_0 a} \cos \frac{\pi}{a} x' \quad (2.12)$$

using Eqs.(2.8) and (2.11), one should define the normal vector of the surface, which can be introduced as

$$\vec{n} = \vec{e}_y \quad (2.13)$$

according to the geometry in Fig.(2-1), to be able to calculate the electrical surface current density [12] can be expressed as

$$\vec{J}_{es} = 2\vec{n} \times \vec{H}_a|_s \quad (2.14)$$

and can be calculated as

$$\vec{J}_{es} = 2\vec{e}_y \times \left(\vec{e}_x \frac{E_i}{Z_0} \sin \frac{\pi}{a} x' + \vec{e}_y \frac{\pi E_i}{jkZ_0 a} \cos \frac{\pi}{a} x' \right) \Big|_{y=0} \quad (2.15)$$

$$\vec{J}_{es} = \vec{e}_z \frac{2E_i}{Z_0} \sin \frac{\pi}{a} x' \quad (2.16)$$

where \vec{J}_{es} is flowing on the parallel plates, induced by the incident electromagnetic field radiating from the source. Consequently, electrical vector potential is calculated using the following formulas;

$$\vec{A} = \frac{\mu_0}{4\pi} \iiint_{v'} \vec{J}_{es}(\vec{r}') \frac{e^{-jkR}}{R} dv' \quad (2.17)$$

by placing the Eq.(2.16) respectively into Eq.(2.17), one obtains

$$\vec{A} = \vec{e}_z \frac{\mu_0 E_i}{2\pi Z_0} \int_{z'=-\infty}^{\infty} \int_{x'=-a}^a \sin \frac{\pi}{a} x' \frac{e^{-jkR}}{R} dx' dz' \quad (2.18)$$

these vector potentials using aperture boundaries. The common double integral in Eq.(2.18) of

$$I_1 = \int_{z'=-\infty}^{\infty} \int_{x'=-a}^a \sin \frac{\pi}{a} x' \frac{e^{-jkR}}{R} dx' dz' \quad (2.19)$$

can be simplified by grouping the functions in integrals as

$$I_1 = \int_{x'=-a}^a \sin \frac{\pi}{a} x' \left(\int_{z'=-\infty}^{\infty} \frac{e^{-jkR}}{R} dz' \right) dx' \quad (2.20)$$

and can be solved. Firstly, z' part of Eq.(2.20) will be solved. Consider this part as

$$I_{11} = \int_{z'=-\infty}^{\infty} \frac{e^{-jkR}}{R} dz' \quad (2.21)$$

where R is equal to

$$R = \sqrt{(x - x')^2 + y^2 + (z - z')^2} \quad (2.22)$$

because of the aperture $y' = 0$. Then consider a new variable R' as

$$R' = \sqrt{(x - x')^2 + y^2} \quad (2.23)$$

Equation (2.22) can be rewritten as

$$R = \sqrt{(R')^2 + (z - z')^2} \quad (2.24)$$

according to the Eq.(2.23). By using the variable change of

$$z - z' = R' \sinh \alpha \quad (2.25)$$

where \sinh represents the hyperbolic sine function, and by calculating the derivative of z' as

$$dz' = -R' \cosh \alpha d\alpha \quad (2.26)$$

R can be calculated as

$$R = \sqrt{(R')^2 + (R')^2(\sinh^2 \alpha)} = R' \sqrt{1 + \sinh^2 \alpha} = R' \cosh \alpha \quad (2.27)$$

then, the common integral in Eq.(2.21) can be calculated as

$$I_{11} = - \int_c \frac{e^{-jkR' \cosh \alpha}}{R' \cosh \alpha} R' \cosh \alpha d\alpha \quad (2.28)$$

Using $R' \rightarrow R$, and simplifying the Eq.(2.28), it is apparent to be able to achieve

$$I_{11} = - \int_c e^{-jkR \cosh \alpha} d\alpha \quad (2.29)$$

where \int_c is a line integral over a c length line. This integral gives a Hankel function a

$$I_{11} = -\frac{\pi}{j} H_0^{(2)}(kR) \quad (2.30)$$

by using the variable change of $(z - z') = R \sinh \alpha$ where R is equal to $\sqrt{(x - x')^2 + y^2}$. As a result one obtains

$$I_{11} = -\frac{\pi}{j} H_0^{(2)}(kR) \cong -\frac{\pi}{j} \sqrt{\frac{2}{\pi}} e^{j\frac{\pi}{4}} \frac{e^{-jkR}}{\sqrt{kR}} \quad (2.31)$$

then the common double integral is reduced to a single integral, and can be written as

$$I_1 = - \int_{x'=-a}^a \sin \frac{\pi}{a} x' \frac{\pi}{j} \sqrt{\frac{2}{\pi}} e^{j\frac{\pi}{4}} \frac{e^{-jkR}}{\sqrt{kR}} dx' \quad (2.32)$$

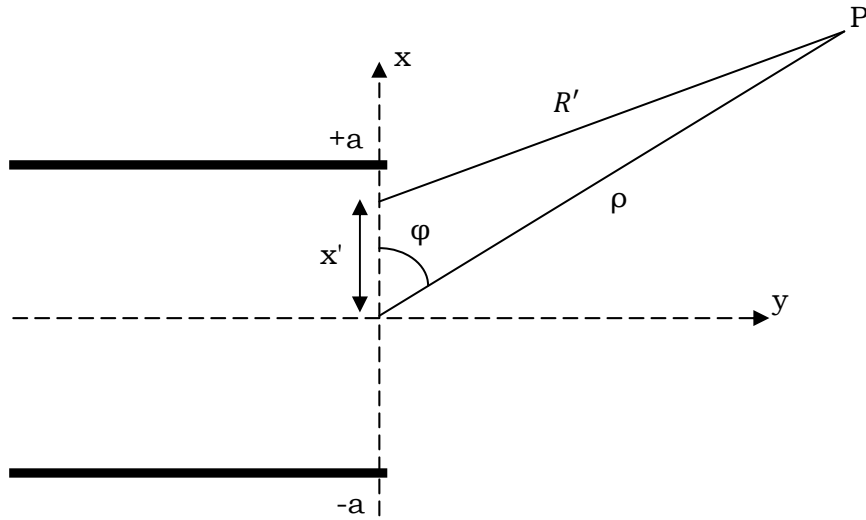


Figure 2.2. Aperture geometry.

Consider a filament of current along the x –axis and located near the origin. Radiation fields will not vary with θ . This because as the observer moves around the source such that ρ and x are constant, the appearance of the source remains the same; thus, its radiation fields are also unchanged. Therefore, for simplicity we will confine the observation point to a fixed θ in the xy –plane ($\theta=90^\circ$) as shown in Fig.(2-2). Using $R \rightarrow R'$, and R' can be calculated as

$$R' = [(x - x')^2 + y^2]^{1/2} \quad (2.33)$$

according to geometry in Fig.(2-2).

$$R' = [x^2 + y^2 + (x')^2 - 2xx']^{1/2} \quad (2.34)$$

$$R' = [\rho^2 + (x')^2 - 2\rho x' \cos \varphi]^{1/2} \quad (2.35)$$

In order to develop approximate expressions for R' , and can be expanded Eq.(2.35) using the binomial theorem;

$$\begin{aligned}
R' &= (\rho^2)^{1/2} + \frac{1}{2}(\rho^2)^{-1/2}[-2\rho x' \cos \varphi + (x')^2] \\
&\quad + \frac{1}{2} \left(\frac{-1}{2} \right) (\rho^2)^{-3/2} [-2\rho x' \cos \varphi + (x')^2]^2 + \dots \\
&= \rho - x' \cos \varphi + \frac{(x')^2 \sin^2 \varphi}{2\rho} + \frac{(x')^3 \sin^2 \varphi \cos \varphi}{2\rho^2} + \dots
\end{aligned} \tag{2.36}$$

The terms in this series decrease as the power of x' increases if x' is small compared to ρ . This expression for R' is used in the radiation integral Eq.(2.32) to different degrees of approximation. In the denominator (which affects only the amplitude), can be written as

$$R' \approx \rho \tag{2.37}$$

The integral Eq.(2.32) sums the contributions from all the points along the line source. Although the amplitude of waves due to each source point is essentially the same, the phase can be different if the path length differences are a sizable fraction of a wavelength. Therefore can be included the first two terms of the series in Eq.(2.36) for the R' in the numerator of Eq.(2.32), giving

$$R' \approx \rho - x' \cos \varphi \tag{2.38}$$

Using the far-field approximations Eq.(2.37) and Eq.(2.38) in Eq.(2.32) yields

$$I_1 = -\frac{\pi}{j} \sqrt{\frac{2}{\pi}} e^{j\frac{\pi}{4}} \int_{x'=-a}^a \sin \frac{\pi}{a} x' \frac{e^{-jk(\rho-x' \cos \varphi)}}{\sqrt{k\rho}} dx' \tag{2.39}$$

Equation (2.39) can be simplified as

$$I_1 = -\frac{\sqrt{2\pi}}{j} e^{j\frac{\pi}{4}} \frac{e^{-jk\rho}}{\sqrt{k\rho}} \int_{x'=-a}^a \sin \frac{\pi}{a} x' e^{jkx' \cos \varphi} dx'. \quad (2.40)$$

Integral part of Eq.(2.40) will be solved. Consider this part as

$$K = \int_{x'=-a}^a \sin \frac{\pi}{a} x' e^{jkx' \cos \varphi} dx' \quad (2.41)$$

where $\sin \frac{\pi}{a} x'$ represents the hyperbolic relation, and can be written as

$$\sin \frac{\pi}{a} x' = \frac{1}{2j} (e^{jx'\pi/a} - e^{-jx'\pi/a}) \quad (2.42)$$

by placing the Eq.(2.42) into Eq.(2.41), one obtains

$$K = \frac{1}{2j} \int_{x'=-a}^a (e^{jx'\pi/a} - e^{-jx'\pi/a}) e^{jkx' \cos \varphi} dx' \quad (2.43)$$

can be simplified by grouping the functions in integral as

$$K = \frac{1}{2j} \left[\int_{x'=-a}^a e^{jx'(k \cos \varphi + \pi/a)} dx' - \int_{x'=-a}^a e^{jx'(k \cos \varphi - \pi/a)} dx' \right] \quad (2.44)$$

and can be solved as

$$K = \frac{1}{2j} \left[\frac{1}{j(k \cos \varphi + \pi/a)} e^{jx'(k \cos \varphi + \pi/a)} \Big|_{x'=-a}^a - \frac{1}{j(k \cos \varphi - \pi/a)} e^{jx'(k \cos \varphi - \pi/a)} \Big|_{x'=-a}^a \right] \quad (2.45)$$

then, the boundary values of common integral in Eq.(2.45) can be calculated as

$$K = \frac{1}{2j} \left[\frac{1}{j(k \cos \varphi + \pi/a)} (e^{j(ka \cos \varphi + \pi)} - e^{-j(ka \cos \varphi + \pi)}) - \frac{1}{j(k \cos \varphi - \pi/a)} (e^{j(ka \cos \varphi - \pi)} - e^{-j(ka \cos \varphi - \pi)}) \right] \quad (2.46)$$

where $\frac{1}{2j} (e^{j(ka \cos \varphi \mp \pi)} - e^{-j(ka \cos \varphi \mp \pi)})$ represents the hyperbolic relation, and can be written as

$$\frac{1}{2j} (e^{j(ka \cos \varphi \mp \pi)} - e^{-j(ka \cos \varphi \mp \pi)}) = \sin (ka \cos \varphi \mp \pi) \quad (2.47)$$

by placing the Eq.(2.47) into Eq.(2.46), one obtains

$$K = \frac{\sin (ka \cos \varphi + \pi)}{j(k \cos \varphi + \pi/a)} - \frac{\sin (ka \cos \varphi - \pi)}{j(k \cos \varphi - \pi/a)} \quad (2.48)$$

Equation (2.40) can be rewritten as

$$I_1 = -\frac{\sqrt{2\pi}}{j} e^{j\frac{\pi}{4}} \frac{e^{-jk\rho}}{\sqrt{k\rho}} \left[\frac{\sin (ka \cos \varphi + \pi)}{j(k \cos \varphi + \pi/a)} - \frac{\sin (ka \cos \varphi - \pi)}{j(k \cos \varphi - \pi/a)} \right] \quad (2.49)$$

and by placing the Eq.(2.49) respectively into Eq.(2.18), one obtains

$$\vec{A} = \vec{e}_z \frac{\mu_0 E_i}{2\pi Z_0} \frac{\sqrt{2\pi}}{j} e^{j\frac{\pi}{4}} \frac{e^{-jk\rho}}{\sqrt{k\rho}} \left[\frac{\sin (ka \cos \varphi + \pi)}{j(k \cos \varphi + \pi/a)} - \frac{\sin (ka \cos \varphi - \pi)}{j(k \cos \varphi - \pi/a)} \right]. \quad (2.50)$$

The scattered field can be introduced as

$$\vec{E} \approx -j\omega \vec{A} \quad (2.51)$$

and can be calculated as

$$\vec{E} = -\vec{e}_z \frac{\mu_0 \omega E_i \sqrt{2\pi}}{2\pi Z_0} e^{j\frac{\pi}{4}} \frac{e^{-jk\rho}}{\sqrt{k\rho}} \left[\frac{\sin(ka \cos \varphi + \pi)}{j(k \cos \varphi + \pi/a)} - \frac{\sin(ka \cos \varphi - \pi)}{j(k \cos \varphi - \pi/a)} \right]. \quad (2.52)$$

CHAPTER 3

SCATTERING FROM IMPEDANCE SLIT

3.1. Scattering Mechanisms

In this problem geometry is seen in Fig. 3.1.

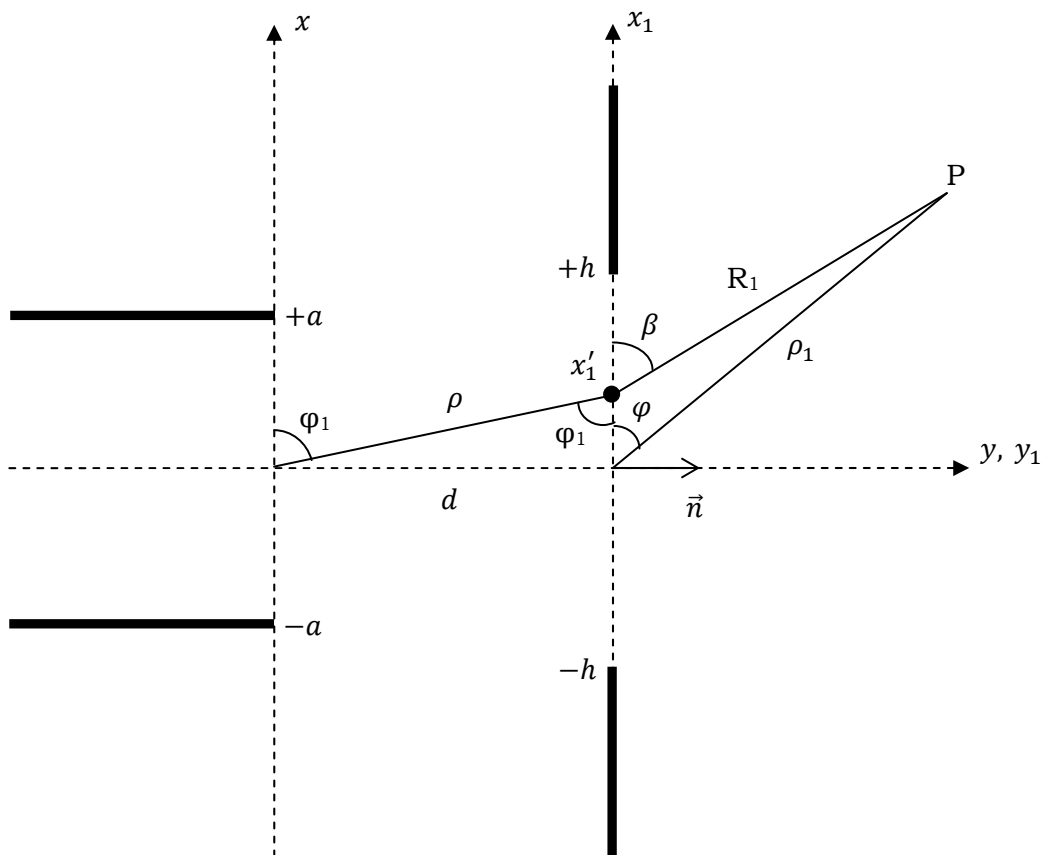


Figure 3.1. Geometry of second problem.

All of the variables and constants are defined in the Charter 2. ρ is equal to $R_1 = [d^2 + (x'_1)^2]^{1/2}$ and φ is equal to $\varphi_1 = \frac{\pi}{2} - \tan^{-1} \frac{x'_1}{d}$ in this geometry.

2.2. PO Solution of the Problem

Incident electrical field can be written as

$$\begin{aligned} \vec{E}_i = & -\vec{e}_z \frac{\mu_0 \omega E_i \sqrt{2\pi}}{2\pi j Z_0} e^{j\frac{\pi}{4}} \frac{e^{-jk[d^2 + (x'_1)^2]^{1/2}}}{\sqrt{k[d^2 + (x'_1)^2]^{1/2}}} \\ & \times \left[\frac{\sin\left(ka \cos\left(\frac{\pi}{2} - \tan^{-1} \frac{x'_1}{d}\right) + \pi\right)}{k \cos\left(\frac{\pi}{2} - \tan^{-1} \frac{x'_1}{d}\right) + \pi/a} \right. \\ & \left. - \frac{\sin\left(ka \cos\left(\frac{\pi}{2} - \tan^{-1} \frac{x'_1}{d}\right) - \pi\right)}{k \cos\left(\frac{\pi}{2} - \tan^{-1} \frac{x'_1}{d}\right) - \pi/a} \right] \end{aligned} \quad (3.1)$$

An integral expression for the incident scattered fields must also be constructed according to the first axiom of MTPO [10]. A semi-infinite aperture can be defined for pseudo-equivalent surface currents can be written on the semi-infinite aperture as

$$\vec{J}_{ms} = -2\vec{n} \times \vec{E}_i|_S, \quad (3.2)$$

where n is unit vector which can be expressed as $\vec{n} = \vec{e}_y$ and the incident scattered field can be obtained from the formula of

$$\vec{F} = \frac{\varepsilon_0}{4\pi} \iiint_{v'} \vec{J}_{ms}(\vec{r}') \frac{e^{-jkR}}{R} dv' \quad (3.3)$$

by placing the Eq.(3.2) respectively into Eq.(3.3), one obtains

$$\begin{aligned} \vec{F} = \vec{e}_x \frac{\mu_0 \varepsilon_0 \omega E_i \sqrt{2\pi}}{8\pi^2 Z_0} e^{j\frac{\pi}{4}} \int_{z'_1=-\infty}^{\infty} \int_{x'_1=-h}^h \frac{e^{-jk[d^2+(x'_1)^2]^{1/2}}}{\sqrt{k[d^2+(x'_1)^2]^{1/2}}} \\ \times \left[\frac{\sin\left(ka \cos\left(\frac{\pi}{2} - \tan^{-1} \frac{x'_1}{d}\right) + \pi\right)}{k \cos\left(\frac{\pi}{2} - \tan^{-1} \frac{x'_1}{d}\right) + \pi/a} - \frac{\sin\left(ka \cos\left(\frac{\pi}{2} - \tan^{-1} \frac{x'_1}{d}\right) - \pi\right)}{k \cos\left(\frac{\pi}{2} - \tan^{-1} \frac{x'_1}{d}\right) - \pi/a} \right] \\ \times \frac{e^{-jkR}}{R} dx'_1 dz'_1. \end{aligned} \quad (3.4)$$

These vector potentials using aperture boundaries. The common double integral in Eq.(3.4) of

$$\begin{aligned} I_2 = \int_{z'_1=-\infty}^{\infty} \int_{x'_1=-h}^h \frac{e^{-jk[d^2+(x'_1)^2]^{1/2}}}{\sqrt{k[d^2+(x'_1)^2]^{1/2}}} \left[\frac{\sin\left(ka \cos\left(\frac{\pi}{2} - \tan^{-1} \frac{x'_1}{d}\right) + \pi\right)}{k \cos\left(\frac{\pi}{2} - \tan^{-1} \frac{x'_1}{d}\right) + \pi/a} \right. \\ \left. - \frac{\sin\left(ka \cos\left(\frac{\pi}{2} - \tan^{-1} \frac{x'_1}{d}\right) - \pi\right)}{k \cos\left(\frac{\pi}{2} - \tan^{-1} \frac{x'_1}{d}\right) - \pi/a} \right] \frac{e^{-jkR}}{R} dx'_1 dz'_1 \end{aligned} \quad (3.5)$$

z'_1 part of Eq.(3.5) will be solved. Consider this part as

$$I_{21} = \int_{z'_1=-\infty}^{\infty} \frac{e^{-jkR}}{R} dz'_1. \quad (3.6)$$

This integral is simplified from Eqs.(2.22) to (2.30) and gives a Hankel function as

$$I_{21} = -\frac{\pi}{j} H_0^{(2)}(kR) \quad (3.7)$$

where general formula of the Hankel function is can be defined as

$$I_{21} = -\frac{\pi}{j} H_0^{(2)}(kR) \cong -\frac{\pi}{j} \sqrt{\frac{2}{\pi}} e^{j\frac{\pi}{4}} \frac{e^{-jkR}}{\sqrt{kR}}. \quad (3.8)$$

Then, the common integral is reduced to a single integral as

$$I_2 = - \int_{x'_1=-h}^h \frac{e^{-jk[d^2+(x'_1)^2]^{1/2}}}{\sqrt{k[d^2+(x'_1)^2]^{1/2}}} \left[\frac{\sin(ka \cos(\frac{\pi}{2} - \tan^{-1} \frac{x'_1}{d}) + \pi)}{k \cos(\frac{\pi}{2} - \tan^{-1} \frac{x'_1}{d}) + \pi/a} \right. \\ \left. - \frac{\sin(ka \cos(\frac{\pi}{2} - \tan^{-1} \frac{x'_1}{d}) - \pi)}{k \cos(\frac{\pi}{2} - \tan^{-1} \frac{x'_1}{d}) - \pi/a} \right] \frac{\pi}{j} \sqrt{\frac{2}{\pi}} e^{j\frac{\pi}{4}} \frac{e^{-jkR}}{R} dx'_1. \quad (3.9)$$

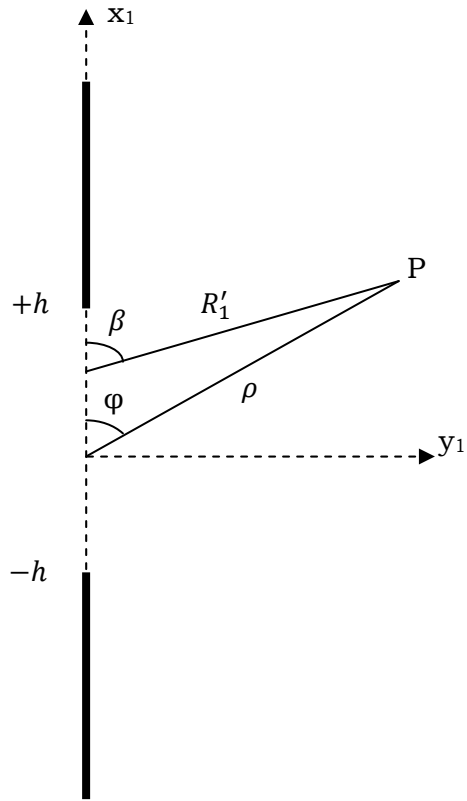


Figure 3.2. Geometry of the impedance slit.

according to geometry in Fig. 3.2. Using $R \rightarrow R'_1$, and R'_1 can be calculated as

$$R'_1 = [(x_1 - x'_1)^2 + y_1^2]^{1/2} \quad (3.10)$$

$$R'_1 = [x_1^2 + y_1^2 + (x'_1)^2 - 2x_1x'_1]^{1/2} \quad (3.11)$$

$$R'_1 = [\rho^2 + (x'_1)^2 - 2\rho x'_1 \cos \varphi]^{1/2} \quad (3.12)$$

$$R'_1 = \rho \left[1 - \frac{2x'_1 \cos \varphi}{\rho} \right]^{1/2} \quad (3.13)$$

and R'_1 can be calculated as

$$R'_1 \cong \rho \left[1 - \frac{x'_1 \cos \varphi}{\rho} \right]. \quad (3.14)$$

The phase function $g_1(x')$ and amplitude function $f_1(x')$ of the Eq.(2.37) can be written as

$$g_1(x') = \rho - x' \cos \varphi \quad (3.17)$$

$$f_1(x') = \rho \quad (3.18)$$

then, the common integral in Eq.(3.9) can be calculated as

$$I_2 = -\frac{\sqrt{2\pi}}{j} e^{j\frac{\pi}{4}} \int_{x'_1=-h}^h \frac{e^{-jk[d^2+(x'_1)^2]^{1/2}}}{\sqrt{k[d^2+(x'_1)^2]^{1/2}}} \times \left[\frac{\sin \left(ka \cos \left(\frac{\pi}{2} - \tan^{-1} \frac{x'_1}{d} \right) + \pi \right)}{k \cos \left(\frac{\pi}{2} - \tan^{-1} \frac{x'_1}{d} \right) + \pi/a} \right. \\ \left. - \frac{\sin \left(ka \cos \left(\frac{\pi}{2} - \tan^{-1} \frac{x'_1}{d} \right) - \pi \right)}{k \cos \left(\frac{\pi}{2} - \tan^{-1} \frac{x'_1}{d} \right) - \pi/a} \right] \frac{e^{-jk(\rho-x'_1 \cos \varphi)}}{\sqrt{k\rho}} dx'_1 \quad (3.19)$$

and by placing the Eq.(3.19) respectively into Eq.(3.4), one obtains

$$\begin{aligned}
\vec{F} = & -\vec{e}_x \frac{\mu_0 \varepsilon_0 \omega E_i e^{j(\frac{\pi}{2}-k\rho)}}{4\pi j Z_0 \sqrt{k\rho}} \int_{x'_1=-h}^h \frac{e^{-jk[d^2+(x'_1)^2]^{1/2}}}{\sqrt{k[d^2+(x'_1)^2]^{1/2}}} \\
& \times \left[\frac{\sin(ka \cos(\frac{\pi}{2}-\tan^{-1}\frac{x'_1}{d}) + \pi)}{k \cos(\frac{\pi}{2}-\tan^{-1}\frac{x'_1}{d}) + \pi/a} \right. \\
& \left. - \frac{\sin(ka \cos(\frac{\pi}{2}-\tan^{-1}\frac{x'_1}{d}) - \pi)}{k \cos(\frac{\pi}{2}-\tan^{-1}\frac{x'_1}{d}) - \pi/a} \right] e^{jkx'_1 \cos \varphi} dx'_1.
\end{aligned} \tag{3.20}$$

The incident scattered field can be introduced as

$$\vec{H} \approx -j\omega F \tag{3.21}$$

and can be calculated as

$$\begin{aligned}
\vec{H} = & \vec{e}_x \frac{k\varepsilon_0 \omega E_i e^{j(\frac{\pi}{2}-k\rho)}}{4\pi \sqrt{k\rho}} \int_{x'_1=-h}^h \frac{e^{-jk[d^2+(x'_1)^2]^{1/2}}}{\sqrt{k[d^2+(x'_1)^2]^{1/2}}} \\
& \times \left[\frac{\sin(ka \cos(\frac{\pi}{2}-\tan^{-1}\frac{x'_1}{d}) + \pi)}{k \cos(\frac{\pi}{2}-\tan^{-1}\frac{x'_1}{d}) + \pi/a} \right. \\
& \left. - \frac{\sin(ka \cos(\frac{\pi}{2}-\tan^{-1}\frac{x'_1}{d}) - \pi)}{k \cos(\frac{\pi}{2}-\tan^{-1}\frac{x'_1}{d}) - \pi/a} \right] e^{jkx'_1 \cos \varphi} dx'_1
\end{aligned} \tag{3.22}$$

Z_0 is the characteristic impedance of the free space and Z is the impedance of the strips. The pseudo-impedance boundary condition in [5] is added to the incident scattered field of Eq.(3.22) in order to construct the total scattered field of the exact solution, which can be written as

$$\begin{aligned}
\vec{H} = \vec{e}_x \frac{k\varepsilon_0\omega E_i e^{j(\frac{\pi}{2}-k\rho)}}{4\pi\sqrt{k\rho}} \int_{x'_1=-h}^h \frac{e^{-jk[d^2+(x'_1)^2]^{1/2}}}{\sqrt{k[d^2+(x'_1)^2]^{1/2}}} \\
\times \left[\frac{\sin\left(ka \cos\left(\frac{\pi}{2}-\tan^{-1}\frac{x'_1}{d}\right) + \pi\right)}{k \cos\left(\frac{\pi}{2}-\tan^{-1}\frac{x'_1}{d}\right) + \pi/a} \right. \\
\left. - \frac{\sin\left(ka \cos\left(\frac{\pi}{2}-\tan^{-1}\frac{x'_1}{d}\right) - \pi\right)}{k \cos\left(\frac{\pi}{2}-\tan^{-1}\frac{x'_1}{d}\right) - \pi/a} \right] \\
\times \frac{Z \sin\left((\varphi + \beta)/2\right) - Z_0}{Z \sin\left((\varphi + \beta)/2\right) + Z_0} e^{jkx'_1 \cos\varphi} dx'_1
\end{aligned} \tag{3.23}$$

Where β is the observation angle. The details of this analysis can be found in [5].

CHAPTER 4

NUMERICAL RESULTS

In this chapter the numerical analysis of the field expressions \vec{E} and \vec{H} will be performed. The scattered field from PEC parallel plate, which is expressed in Eq.(2.52), plots are following pattern for $\lambda = 0.1$, which is the wavelength in meters, $a = 2\lambda$, which is the aperture length.

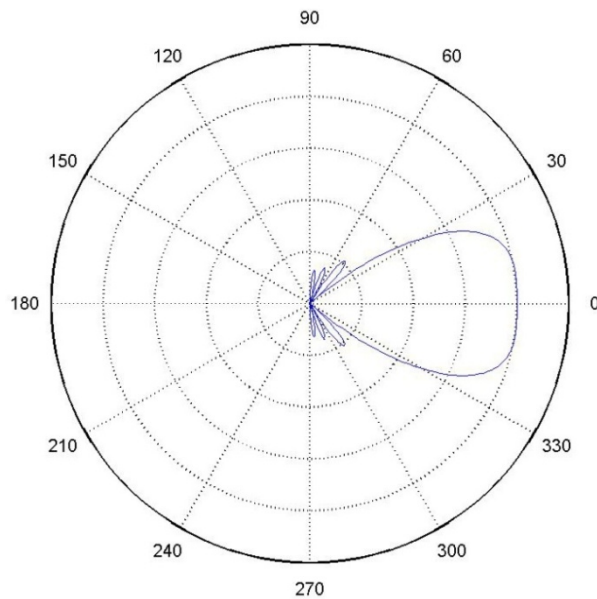
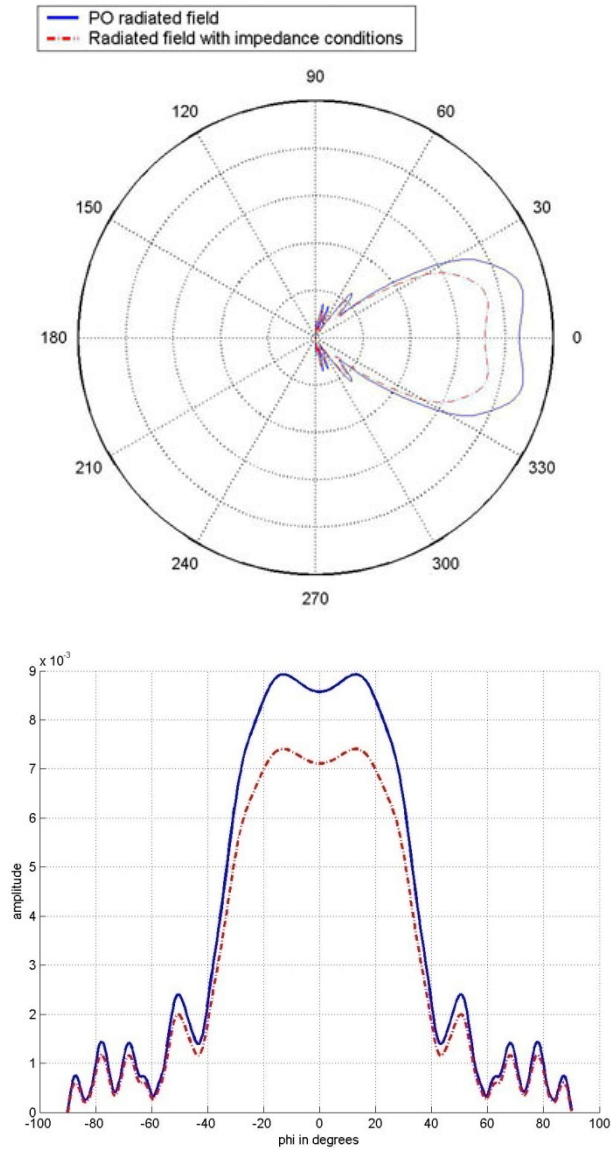


Figure 4.1. Scattered field for geometry of Fig. 2.1.

The power pattern is shown in Fig. 4.1. as a polar plot in linear units. It consists of several lobes. The main lobe is the containing the direction of maximum radiation.

Figure 4.2.(a) and (b) shows the radiated field from impedance slit, which is expressed in Eq.(3.23), plots are following pattern for $\lambda = 0.1$, which is the wavelength in meters, $a = 2\lambda$, which is the aperture length, $d = 1\lambda$, which is the length between parallel plate and slit, $h = 6\lambda$, which is the slit length. The angle of incidence is taken as $\pi/6$ and Z_0/Z has the value of 10.



$$a = 2\lambda, d = 1\lambda, h = 6\lambda$$

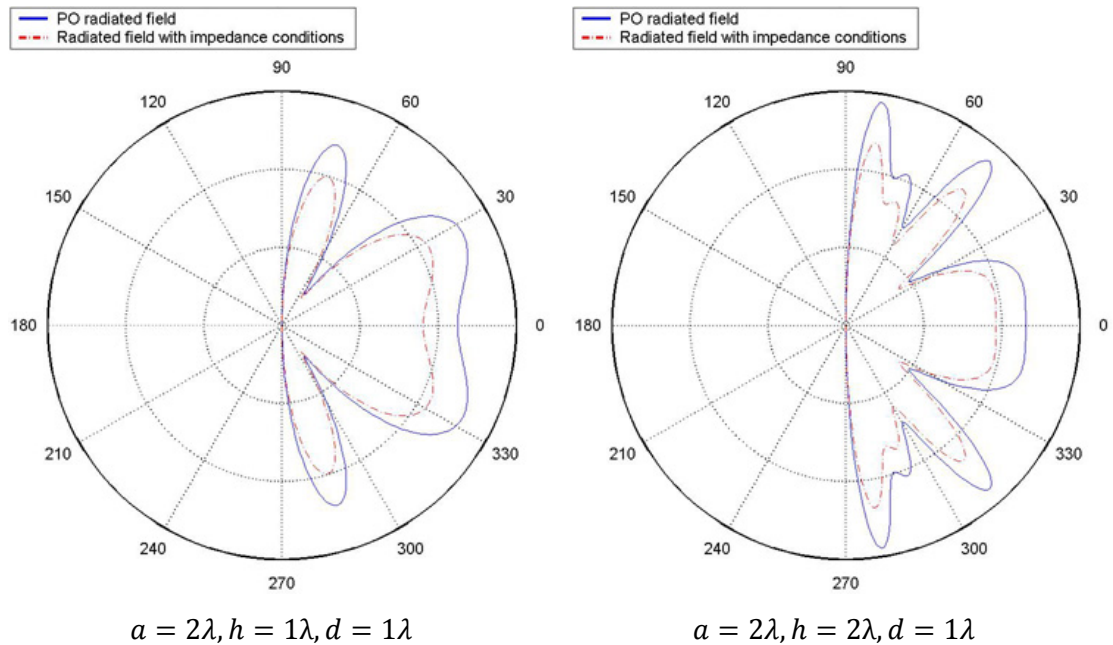
Figure 4.2. The effect of impedance half planes to the radiating fields for the geometry of Fig. 3.1.

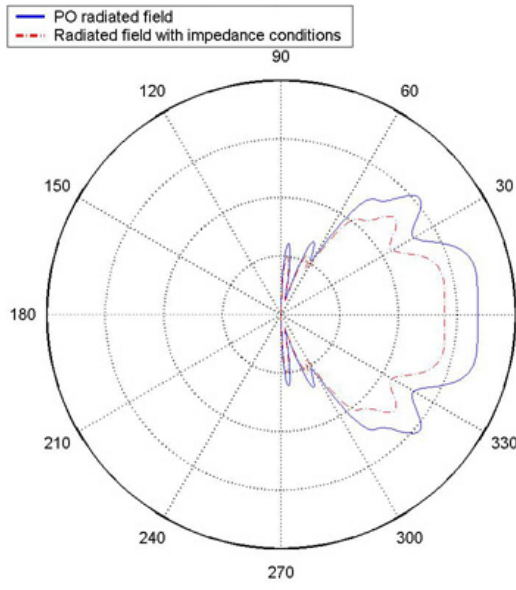
Horizontal coordinate shows the observation angle φ in degrees, and vertical coordinate shows the relative amplitude of the field which is expressed in the figure.

The effect of the impedance boundary conditions on the geometry of Fig. 3.1 can be seen above Fig. 4.2. The difference between the patterns which is illustrated solid line and dashed in Fig. 4.2 is caused by impedance boundary conditions.

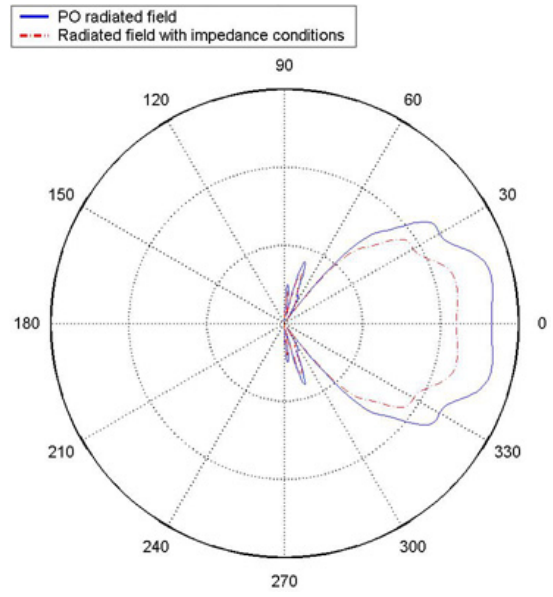
In Fig. 4.2, It can be seen that amplitude is decreasing with the effect of impedance boundary conditions.

It is mentioned that variation with aperture, radiated field, aperture length and length between parallel plate and slit are showing below in Figs. 4.3 and 4.4.

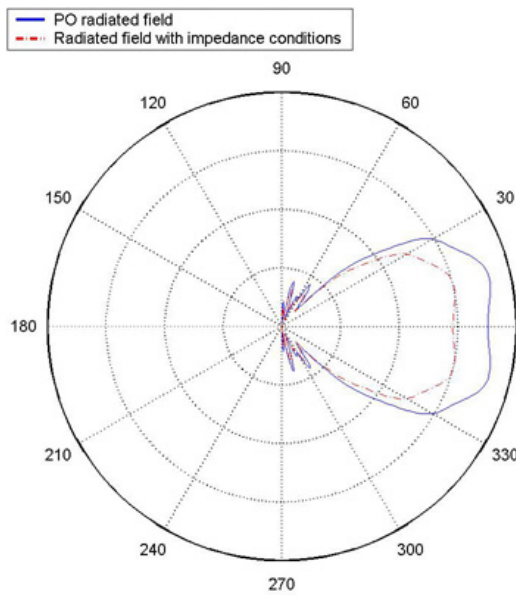




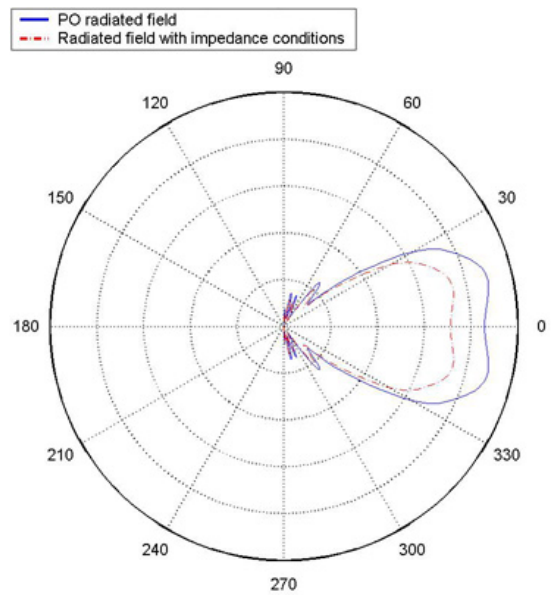
$$a = 2\lambda, h = 3\lambda, d = 1\lambda$$



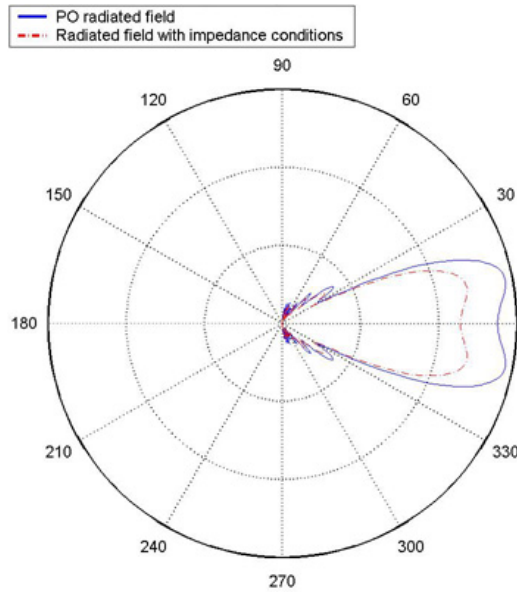
$$a = 2\lambda, h = 4\lambda, d = 1\lambda$$



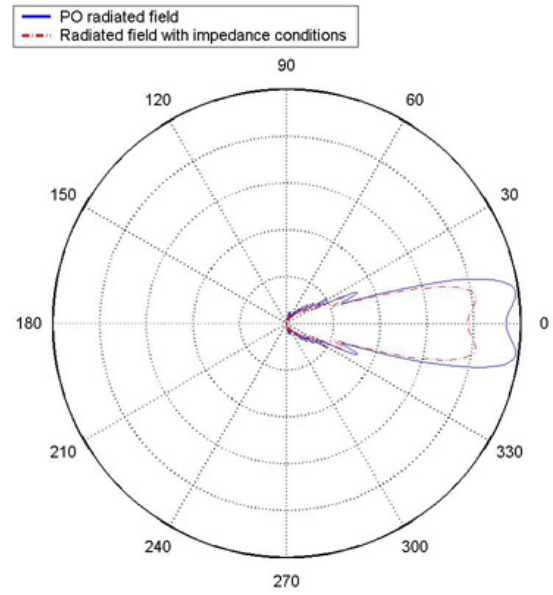
$$a = 2\lambda, h = 5\lambda, d = 1\lambda$$



$$a = 2\lambda, h = 6\lambda, d = 1\lambda$$

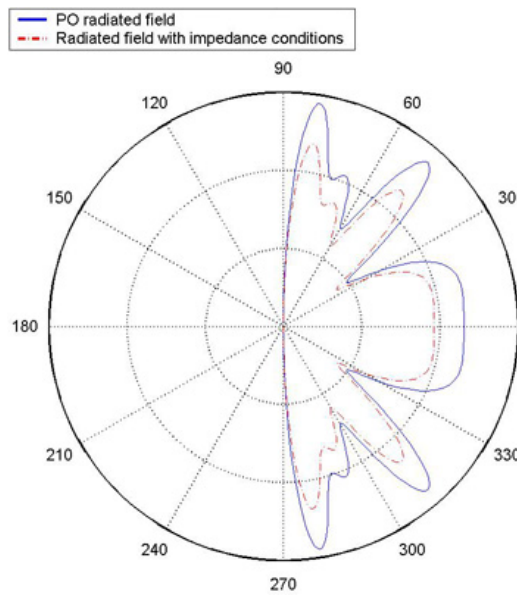


$$a = 2\lambda, h = 10\lambda, d = 1\lambda$$

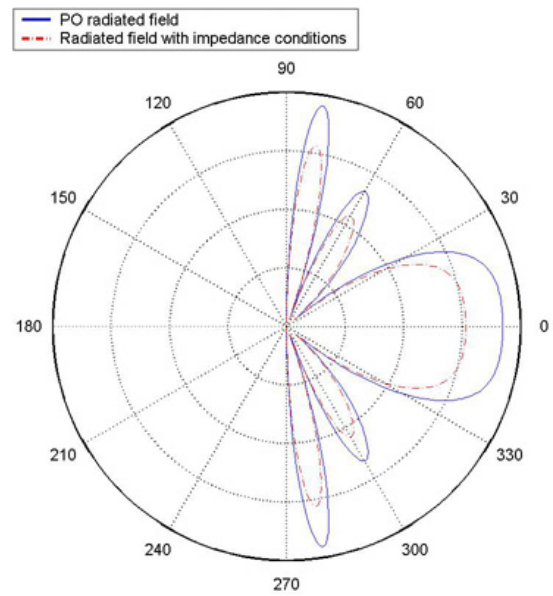


$$a = 2\lambda, h = 20\lambda, d = 1\lambda$$

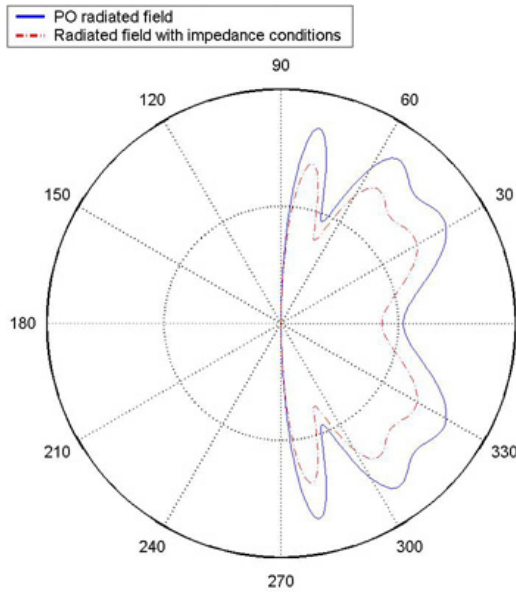
Figure 4.3. Radiated field for geometry of Fig. 3.1.



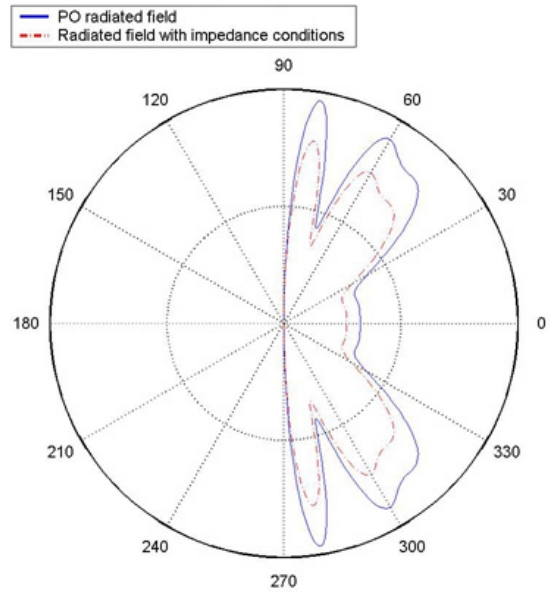
$$a = 2\lambda, h = 2\lambda, d = 1\lambda$$



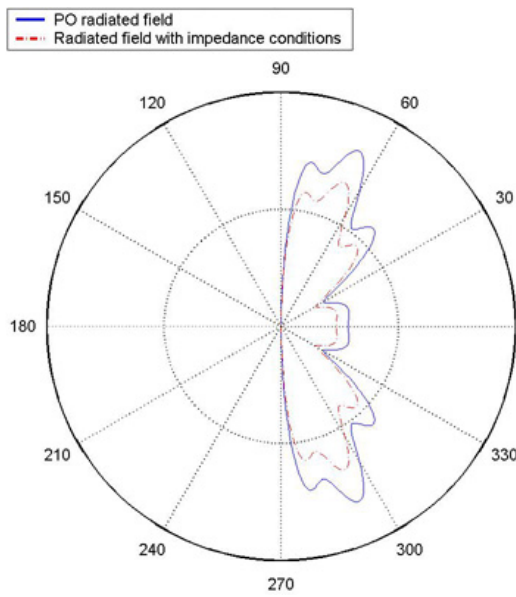
$$a = 2\lambda, h = 2\lambda, d = 2\lambda$$



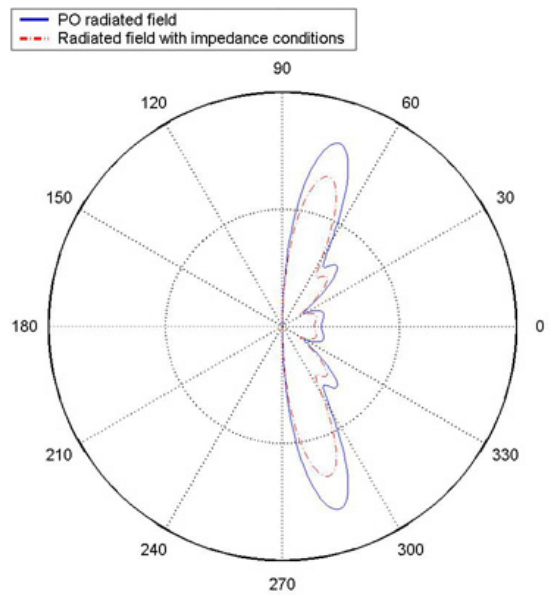
$$a = 2\lambda, h = 2\lambda, d = 3\lambda$$



$$a = 2\lambda, h = 2\lambda, d = 4\lambda$$



$$a = 2\lambda, h = 2\lambda, d = 5\lambda$$



$$a = 2\lambda, h = 2\lambda, d = 6\lambda$$

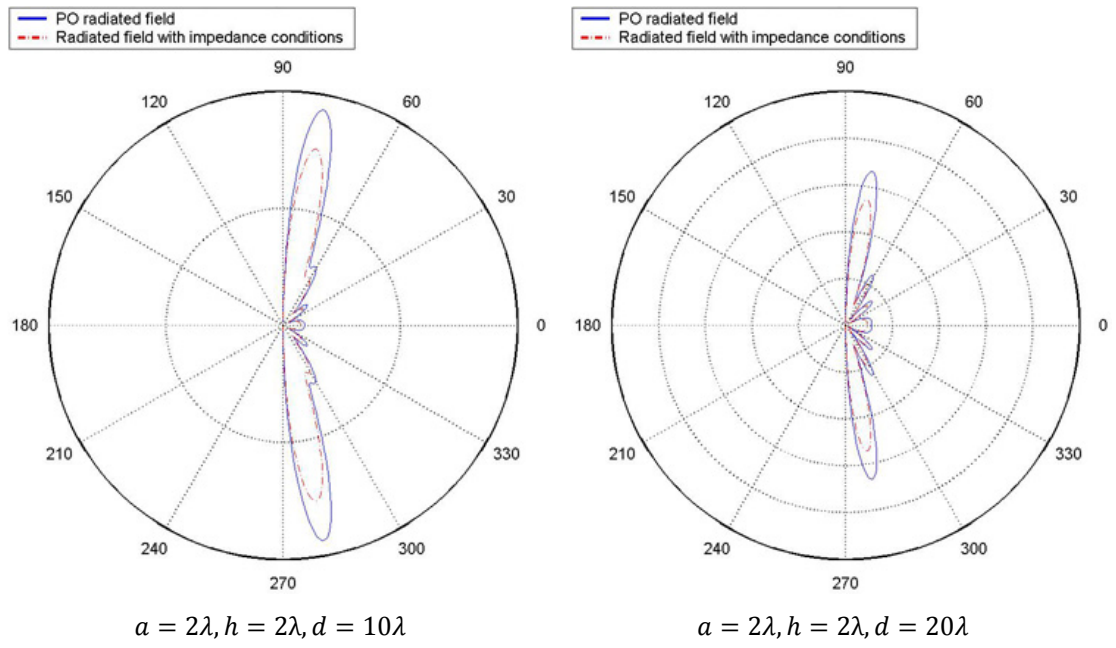


Figure 4.4. Radiated field for geometry of Fig. 3.1.

CHAPTER 5

CONCLUSIONS

In this thesis, we examine the process of slits and strips diffraction on the impedance boundary conditions by using PO and MTPO methods.

The effect of impedance boundary conditions on the geometry of chapter 3 is discussed in this chapter according to the figures in chapter 4.

As it seen in Fig. 4.3, the term of being stable with length between parallel plate and aperture, when aperture length is increased, impedance boundary conditions are decreased as well. And the patterns of radiated field from aperture are approaching the patterns of radiated field from parallel plate.

In Fig. 4.4, when the length between parallel plate and aperture is increased, it is seen that side lobes are expanded as the same time.

REFERENCES

- [1] **McNAMARA, D. A., PISTORIUS, C. W. I., MALHERBE, J. A. G.,** (1990), *Introduction to The Uniform Geometrical Theory of Diffraction*, Artech House, Boston.

- [2] **PATHAK, P. H.,** (1993), *Techniques for High Frequency Problems*, *Antenna Handbook*, Van Nostrand Reinhold, New York.

- [3] **HANSEN, T. B.,** (1991), Corner Diffraction Coefficients for the quarter plate, *IEEE Trans. Antennas Propag.*, vol. 39, no.7

- [4] **STUTZMAN, W.L., THIELE, G.A.** (1998), *Antenna Theory and Design*, John Wiley & Sons, Inc.

- [5] **UMUL, Y.Z.,** (2006), Modified Theory of Physical Optics Solution of Impedance Half Plane Problem, *IEEE Trans. Antennas Propag.*, vol. 54, no.7

- [6] **UFIMTSEV, P. Y.,** (1971), Method of Edge Waves in the Physical Theory of Diffraction translation prepared by the U.S. Air Force Foreign Tech.Div. OH, *Wright Patterson AFB*.

- [7] **UFIMTSEV, P. Y.**, (1989), Theory of Acoustical Edge Waves, *J.Acoust. Soc. Am.*, vol. 86.

- [8] **KNOTT, E. F., SENIOR, T. B. A.**, (1974), Comparison of three high-frequency diffraction techniques, *Proc. IEEE*, vol. 62.

- [9] **LEE, S.W.**, (1977), Comparison of uniform asymptotic theory and Ufimtsev's theory of electromagnetic edge diffraction, *IEEE Trans. Antennas Propag.*, vol. 25.

- [10] **UMUL, Y.Z.**, (2004), Modified Theory of Physical Optics, *Opt. Express*, vol. 12

- [11] **HAYT, W.H.Jr., BUCK, J.A.**, (2001), *Engineering Electromagnetics*, McGraw-Hill, 6th ed.

- [12] **BALANIS, C.A.**, (1989), *Advanced Engineering Electromagnetics*, John Wiley & Sons, Inc.

APPENDIX A

MATLAB PROGRAMME FOR GEOMETRY IN CHAPTER 2

```
L=0.1;
k=2.*pi./L;
phi=[-pi./2:0.01:pi./2];
h=2.*L;
n=4;
A11=sin(k.*h.*cos(phi)+n.*pi);
A12=j.*(k.*cos(phi)+(n.*pi./h));
A21=sin(k.*h.*cos(phi)-n.*pi);
A22=j.*(k.*cos(phi)-(n.*pi./h));
K=(A11./A12)-(A21./A22);
%plot(phi*180/pi,abs(K));
polar(phi,abs(K));
%grid on;
hold on;
clear
```

APPENDIX B

MATLAB PROGRAMME FOR GEOMETRY IN CHAPTER 3

```
%  
%  
N=1000;  
sum=0;  
sum1=0;  
L=0.1;  
k=2.*pi./L;  
phi=[-pi./2:0.01:pi./2];  
rho1=10./k;  
%B=pi./6;  
h=2.*L;  
h1=2.*L;  
d=20.*L;  
n=4;  
Z01=10;  
altsinir=-h1;  
ustsinir=h1;  
delta=(ustsinir-altsinir)./N;  
for i=0:N;  
    x=altsinir+(i.*delta);  
    x1=rho1.*cos(phi);  
    A=1./2;  
    R=((d.^2)+(x.^2)).^(1./2);  
    Beta=acos((x1-x)./R);  
    C1=exp(-j.*k.*R);
```



```

C2=(k.*R).^(1./2);
G1=(pi./2)-atan(x./d);
A11=sin(k.*h.*cos(G1)+n.*pi);
A12=j.*(k.*cos(G1)+(n.*pi./h));
A21=sin(k.*h.*cos(G1)-n.*pi);
A22=j.*(k.*cos(G1)-(n.*pi./h));
Z=sin((G1+Beta)./2);
F1=A.*(C1./C2).*((A11./A12)-(A21./A22)).*exp(j.*k.*x.*cos(phi));
F2=A.*(C1./C2).*((A11./A12)-(A21./A22)).*((Z-
Z01)/(Z+Z01)).*exp(j.*k.*x.*cos(phi));
q=F1;
q1=F2;
sum=sum+q;
sum1=sum1+q1;
end
FA=sum.*delta;
FB=sum1.*delta;
%
%
%figure(1);
%subplot(1,2,1);
polar(phi,abs(FA));
hold on;
polar(phi,abs(FB),'-r');
%s=legend('PO Radiated Field','Radiated Field an Impedance Plane',2);
%
%
hold on;
%subplot(1,2,2);
%plot(phi*180/pi,abs(FA),'LineWidth',2);
%hold on;
%plot(phi*180/pi,abs(FB),'-r','LineWidth',2);
%xlabel('phi in degrees');
%ylabel('amplitude');

```

```
%s=legend('PO Radiated Field','Radiated Field an Impedance Plane',2);  
grid on;  
hold on;  
clear
```